

# Interpretable Automatic Detection of Incomplete Hippocampal Inversions Using Anatomical Criteria

Lisa J. Hemforth, Claire Cury, Kevin De Matos, Alexandre Martin, Vincent Frouin, Sylvane Desrivière, Antoine Grigis, Hugh Garavan, Rüdiger Brühl, Jean-Luc Martinot, Marie-Laure Paillère Martinot, Eric Artiges, Luise Poustka, Sarah Hohmann, Sabina Millenet, Nilakshi Vaidya, Henrik Walter, Robert Whelan, Gunter Schumann, Baptiste Couvy-Duchesne, Olivier Colliot, and The IMAGEN consortium

Sorbonne Université, Institut du Cerveau - Paris Brain Institute - ICM, CNRS, Inria, Inserm, AP-HP, Paris, France; Univ Rennes, CNRS, Inria, Inserm, IRISA UMR 6074, Emrah - ERL U 1228, F-35000 Rennes, France; NeuroSpin, CEA, Université Paris-Saclay, F-91191 Gif-sur-Yvette, France; Medical Faculty Mannheim, Heidelberg University, Square 45, 68159 Mannheim, Germany; Institute of Psychiatry, Psychology & Neuroscience, King's College London, United Kingdom; Departments of Psychiatry and Psychology, University of Vermont, 05405 Burlington, Vermont, USA; Physikalisch-Technische Bundesanstalt (PTB), Braunschweig and Berlin, Germany; INSERM U 110 Université Paris-Saclay, CNRS, Centre Borrel, Gif-sur-Yvette, France; University Medical Centre Göttingen, Göttingen, Germany; Centre for Population Neuroscience and Stratified Medicine (PONS), Charité Universitätsmedizin Berlin, Germany; Universitätsmedizin Berlin, Freie Universität Berlin, Humboldt-Universität zu Berlin, Berlin, Germany; Trinity College Dublin, Ireland; Institute for Science and Technology of Brain-inspired Intelligence (ISTBI), Fudan University, Shanghai, China; Institute for Molecular Bioscience, the University of Queensland, Brisbane, Australia

## Abstract

hemforth@gmail.com

Incomplete Hippocampal Inversion (IHI) is an atypical anatomical pattern of the hippocampus that has been associated with several brain disorders (epilepsy, schizophrenia) <sup>1-5</sup>. IHI can be visually detected on coronal T1 weighted MRI images. IHI can be absent, partial or complete (no IHI, partial IHI, IHI). However, visual evaluation can be long and tedious, justifying the need for an automatic method. In this paper, we propose, to the best of our knowledge, the first automatic IHI detection method from T1-weighted MRI. The originality of our approach is that, instead of directly detecting IHI, we propose to predict several anatomical criteria, which each characterize a particular anatomical feature of IHI, and that can ultimately be combined for IHI detection <sup>6</sup>.

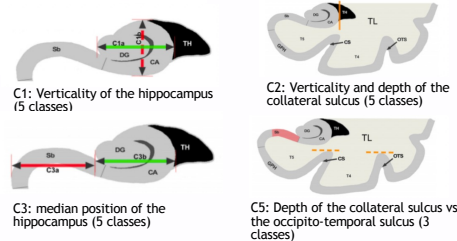


Figure 1. Schematic of criteria 1-5 extracted from 6.

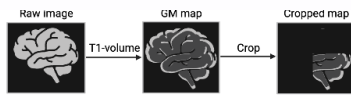
Such individual criteria have the advantage of providing interpretable anatomical information regarding the morphological aspect of a given hippocampus. We relied on a large population of 2,008 participants from the IMAGEN study. The approach is general and can be used with different machine learning models. In this paper, we explored two different backbone models for the prediction: a linear method (ridge regression) and a deep convolutional neural network. We demonstrated that the interpretable, anatomical based prediction was at least as good as when predicting directly the presence of IHI, while providing interpretable information to the clinician or neuroscientist. This approach may be applied to other diagnostic tasks which can be characterized radiologically by several anatomical features

## Methods

### IMAGEN dataset

- 2006 images split into 75/25% train/test set with best similarity in distribution
- Average age of 14 yo.
- 50/50 M/F

### Pre-processing

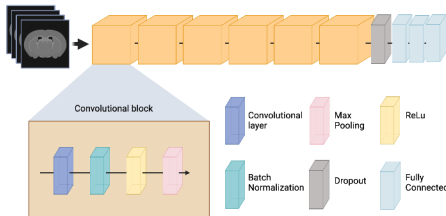


### Models

#### Ridge Regression :

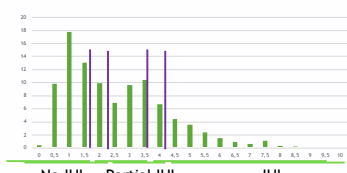
$$\min_{\beta} E(\alpha, \beta) = \sum_{i=1}^n (y_i - X_i \beta)^2 + \alpha \|\beta\|^2$$

#### Conv5-FC3 implemented in ClinicaDL <sup>7</sup>:



#### Conversion to C0

Iteratively used 2 thresholds to separate composite scores (SC) of training set into no-IHI (score of 0), partial IHI (0.5) and IHI (1) and compute balanced accuracy (BA). The thresholds with the best BA was used for the conversion: 2.25 and 4.25)



## Results

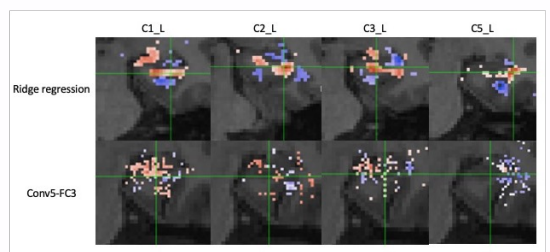
	C1_L	C1_R	C2_L	C2_R	C3_L	C3_R	C5_L	C5_R	SC_{L,R}_{add}	SC_{L,R}_{add}	SC_{L,R}	SC_{L,R}
	Weighted Kappa				Kappa				ICC			
Ridge Regression	0.558 ± 0.027	0.256 ± 0.037	0.675 ± 0.024	0.599 ± 0.019	0.717 ± 0.019	0.627 ± 0.031	0.268 ± 0.031	0.187 ± 0.034	0.684 ± 0.023	0.576 ± 0.031	0.708 ± 0.021	0.633 ± 0.024
Conv5-FC3	0.717 ± 0.022	0.501 ± 0.033	0.749 ± 0.021	0.644 ± 0.028	0.769 ± 0.018	0.694 ± 0.028	0.502 ± 0.031	0.331 ± 0.047	0.811 ± 0.015	0.678 ± 0.032	0.788 ± 0.015	0.703 ± 0.027

Table 1. Performances for the prediction of individual criteria C1, C2, C3, C5 and for the direct prediction of the IHI score (either using the sum of the predictions of individual criteria, denoted as "SC\_{L,R}\_{add}", or using direct prediction of SC, denoted as "SC\_{L,R}"). The table shows the mean ± the standard error computed using bootstrap on the test set. Criteria 1 to 5 are evaluated using a weighted kappa score to make up for their linearity. C5 is evaluated using an unweighted kappa score and the composite scores were evaluated using Inter-Class Correlations. Overall, the deep network outperformed the ridge regression on all tasks.

	C0_L	C0_R	SC_{L,R}_{add}	SC_{L,R}_{add}	SC_{L,R}	SC_{L,R}
Ridge Regression	0.546 ± 0.031	0.500 ± 0.047	0.640 ± 0.027	0.563 ± 0.037	0.628 ± 0.029	0.601 ± 0.033
Conv5-FC3	0.763 ± 0.023	0.668 ± 0.045	0.739 ± 0.023	0.647 ± 0.037	0.740 ± 0.023	0.610 ± 0.043

Table 2. Kappa scores for prediction of C0, either directly, or through thresholding the sum of the predictions of the individual criteria ("SC\_{L,R}\_{add}"), or through thresholding the direct prediction of the IHI score ("SC\_{L,R}"). Mean ± standard error (of each metric), computed using bootstrap on the test set. The models performed better when using individual criteria and composite scores.

Figure 2. Weight maps extracted from ridge regression and saliency maps from the Conv5 FC3 for C1, C2, C3, C5 in the left hemisphere on T1 weighted MRI image. Criteria C1 and C3 which assess the position of the hippocampus highlight its surroundings in both cases and criteria C2 and C5 which deal with sulci positions highlight the latter as expected.



## Conclusion

We have proposed to automatically detect IHI by predicting anatomically interpretable individual criteria. We showed that this approach does not decrease predictive performance compared to directly predicting the presence of IHI. Predicting individual criteria provides much more information about the specific anatomical characteristics underlying the IHI of a given participant, thereby providing more interpretable information to the clinician or neuroscientist. This training strategy has the potential to be applied to other diagnosis tasks which can be characterized by individual interpretable criteria.

## References

- [1] Lehericy, S., Dormont, D., Semah, F., Clémenceau, S., Granat, O., Marsault, C., and Baulac, M., "Developmental abnormalities of the medial temporal lobe in patients with temporal lobe epilepsy," *AJNR Am J Neuroradiol.* 18, 817-828 (1995).
- [2] Baulac, M., De Gissac, N., Hasboun, D., Oppenheim, C., Adam, C., Arzimanoglou, A., Semah, F., Lehericy, S., Clémenceau, S., and Berger, B., "Hippocampal developmental changes in patients with partial epilepsy: magnetic resonance imaging and clinical aspects," *Ann Neurol.* 44, 223-33 (1998).
- [3] Bernasconi, N., Kinay, D., Andermann, F., Antel, S., and Bernasconi, A., "Analysis of shape and positioning of the hippocampal formation: an MRI study in patients with partial epilepsy and healthy controls," *Brain.* 128, 2442-2452 (2005).
- [4] Bajic, D., Kumlien, E., Mattsson, P., Lundberg, S., Wang, C., and Raininko, R., "Incomplete hippocampal inversion - is there a relation to epilepsy?," *Eur Radiol.* 19, 2544-2550 (2009).
- [5] Roeske, M. J., McHugh, M., Vandekar, S., Blackford, J. U., Woodward, N. D., and Heckers, S., "Incomplete hippocampal inversion in schizophrenia: prevalence, severity, and impact on hippocampal structure," *Mol Psychiatry.* 26, 5407-5416 (2021).
- [6] Cury, C., Toro, R., Cohen, F., Fischer, C., Mhaya, A., Samper-Gonzalez, J., Hasboun, D., Mangin, J.-F., Banaschewski, T., Bokde, A. L. W., Bromberg, U., Buechel, C., Cattrell, A., Conrad, P., Flor, H., Gallinat, J., Garavan, H., Gowland, P., Heinz, A., Ittermann, B., Lemaitre, H., Martinot, J.-L., Nees, F., Paillère Martinot, M.-L., Orfanos, D. P., Paus, T., Poustka, L., Smolka, M. N., Walter, H., Whelan, R., Frouin, V., Schumann, G., Glau, S., J. A., Colliot, O., and the IMAGEN Consortium, "Incomplete hippocampal inversion: A comprehensive MRI study of over 2000 subjects," *Front Neuroanat.* 9, 160 (2015).
- [7] Thibeau-Sutre, E., Diaz, M., Hassanaly, R., Routier, A., Dormont, D., Colliot, O., and Burgos, N., "ClinicaDL: an open-source deep learning software for reproducible neuroimaging processing," *Computer Methods and Programs in Biomedicine* 220, 106818 (2022). (2015).